Liquid Crystals
Publication details, including instructions for authors and subscription information:
http://www.informaworld.com/smpp/title~content=t713926090

Numerical methods for light propagation in large LC cells: a new approach

D. Olivero[a]; C. Oldano[a]
[a] Physics Department and INFM, Politecnico di Torino, 24 Corso Duca degli Abruzzi, 10129 Torino, Italy,

Online publication date: 11 November 2010

To cite this Article Olivero, D. and Oldano, C.(2003) 'Numerical methods for light propagation in large LC cells: a new approach', Liquid Crystals, 30: 3, 345 — 353
To link to this Article: DOI: 10.1080/0267829031000080996
URL: http://dx.doi.org/10.1080/0267829031000080996

LIQUID CRYSTALS, 2003, VOL. 30, NO. 3, 345–353

Numerical methods for light propagation in large LC cells: a new approach

D. OLIVERO* and C. OLDANO

Physics Department and INFM, Politecnico di Torino,
24 Corso Duca degli Abruzzi, 10129 Torino, Italy

(*Received 18 March 2002; in final form 29 November 2002; accepted 2 December 2002*)

Accurate numerical methods for the propagation of light in large 3D samples with strong lateral variation of the director field require prohibitive amounts of time. We consider and compare a standard spectral method and the Finite Difference in Frequency Domain method, showing that the CPU time can be reduced by one or two orders of magnitude using a perturbation approach or a recently developed Reduced Order Method. The equations obtained are applied to liquid crystal cells with in-plane switching, illuminated by a large incoherent source. The developed formalism, based on numerically exact equations, is particularly suitable for treating magnetic or optically active media and for extending to such media the well known approximations based on the 4×4 (Berreman) or 2×2 (Jones) matrices.

1. Introduction

The reflection and transmission properties of large samples are considered in the framework of linear optics, with particular attention to liquid crystal (LC) cells between parallel planes. For stratified media, i.e. for cells whose director field $\hat{n}(\vec{r})$ depends only on the coordinate z orthogonal to the boundaries, the incident field can be expanded in plane waves, each one giving rise to a transmitted and to a reflected plane wave, with two independent polarization states. The optical problem can therefore be exactly solved by the 4×4 matrix method [1], known in the LC literature as the Berreman method [2].

For large cells whose director field $\hat{n}$ also depends on the transverse vector $\vec{r}_t$ (3D cells), highly accurate numerical methods require generally prohibitive CPU times and memory, hence the wide use of approximated methods. If the dependence of $\hat{n}$ on $\vec{r}_t$ is smooth on the wavelength scale and the incidence angle is small, it is a good approximation to divide the cell into laterally homogeneous sub-cells, each one treated by the 4×4 matrix method or by methods which neglect multiple reflection and are based on complex 2×2 matrices (Jones calculus [3]) or on real 4×4 matrices (Stokes–Mueller calculus [4]).

We consider here two numerically exact methods, namely a spectral method first developed for gratings, the Grating Method [5], and the Finite Difference in Frequency Domain method, FDFD. The aim of this contribution is to show that for some standard optical problems the CPU time and memory requirements can be greatly reduced by a perturbation expansion or by a recently developed Reduced Order Method [6]. To explain better the difficulties found with large samples and to describe the organization of the paper, let us consider a LC display made of in-plane pixels having lateral dimensions $L = 200\lambda$ ($\approx 100\,\mu m$), with the simplifying assumption $\hat{n} = \hat{n}(x)$, with $\hat{n}(0) = \hat{n}(L)$ (periodic boundary conditions). The Grating Method considers the pixel as the unit cell of a grating periodic along x having a period equal to L. The number of beams generated by an incident plane wave is of the order of $2L/\lambda$, each one described by a 4×4 matrix. The transfer matrix U and the scattering matrix S are therefore defined in a vector space whose dimension is of the order of 1600. The CPU time, with the presently existing PC, is of the order of hours. The FDFD, the Finite Different Time Domain method [7] and the Beam Propagation Method (BPM), that have been recently suggested for LC cells [8], usually require even longer times. For full 3D samples, the dimension of the Hilbert space becomes of the order of 10^6, and there is no hope of solving our problem using the standard versions of such methods. The space dimension and the computer time can be either decreased for smooth director profiles or increased in the absence of periodic boundary conditions, but their order of magnitude cannot be greatly changed. A new approach, different from the standard one, is therefore required.

For a guide to the symbols used in the following, see the appendix.

*Author for correspondence; e-mail: d.olivero@tin.it

Liquid Crystals ISSN 0267-8292 print/ISSN 1366-5855 online © 2003 Taylor & Francis Ltd
http://www.tandf.co.uk/journals
DOI: 10.1080/0267829031000080996

2. Definition of the formalism: Marcuvitz–Schwinger form of Maxwell equations

The material equations defining the optical properties of the medium are written in the Tellegen form [9, 10], and more precisely as:

$$\begin{aligned}\vec{d} &= \varepsilon\vec{e} + \chi\vec{h} \\ \vec{b} &= \eta\vec{e} + \mu\vec{h}\end{aligned} \tag{1}$$

where

$$\begin{aligned}\vec{e} &= Z_0^{-1/2}\vec{E}, \quad \varepsilon_0\vec{d} = Z_0^{-1/2}\vec{D} \\ \vec{h} &= Z_0^{+1/2}\vec{H}, \quad \mu_0\vec{b} = Z_0^{+1/2}\vec{B}.\end{aligned} \tag{2}$$

ε and μ are the relative permittivity and permeability, respectively; χ and η are dimensionless pseudotensors which take into account the possible intrinsic chirality of the medium; and $Z_0 = (\mu_0/\varepsilon_0)^{1/2}$. These equations are particularly suitable for bianisotropic media, but the formalism developed here is also convenient for the usual dielectric media, where $\chi = \eta = 0$ and the relative permeability can be assumed equal to 1.

Let us consider a sample between the planes $z = 0$ and $z = d$. In the frequency domain, the electromagnetic field is defined by the tangential components of $\vec{e}$ and $\vec{h}$, which are written as:

$$(e_x \;\; h_x \;\; e_y \;\; h_y)^{\mathrm{T}} = \psi(\vec{r}_{\mathrm{t}}, z)\cdot\exp[\mathrm{i}(\vec{k}_{\mathrm{t}}\vec{r}_{\mathrm{t}} - \omega t)] \tag{3}$$

where the index t denotes the transverse component and the superscipt T indicates the transpose vector; ψ is a 4-vector whose elements give the amplitudes of the components of the field and $\vec{k}_{\mathrm{t}}$ is chosen to make the dependence of ψ on $\vec{r}_{\mathrm{t}}$ as smooth as possible. If the incident field is a single plane wave, it is convenient to identify $\vec{k}_{\mathrm{t}}$ with the tangential component of the incident wave vector $\vec{k}$.

The time-harmonic Maxwell equations can be written in the Marcuvitz–Schwinger form [11], as

$$\partial_z\psi = \mathrm{i}k_0 J_4 L\psi \tag{4}$$

where

$$L = \gamma_{\mathrm{tt}} - (D_{\mathrm{t}} + N_{\mathrm{t}} + \gamma_{\mathrm{tz}})\gamma_{zz}^{-1}(D_{\mathrm{t}}^{\dagger} + N_{\mathrm{t}}^{\dagger} + \gamma_{\mathrm{zt}}) \tag{5}$$

$$\gamma_{\mathrm{tt}} = \begin{pmatrix}\gamma_{xx} & \gamma_{xy} \\ \gamma_{yx} & \gamma_{yy}\end{pmatrix}, \quad \gamma_{\mathrm{tz}} = \begin{pmatrix}\gamma_{xz} \\ \gamma_{yz}\end{pmatrix}, \quad \gamma_{\mathrm{zt}} = (\gamma_{zx} \;\; \gamma_{zy}) \tag{6}$$

$$\begin{aligned}D_{\mathrm{t}} &= (\mathrm{i}k_0)^{-1}\,\mathrm{kron}(J_2\partial_{\mathrm{t}}, J_2) \\ N_{\mathrm{t}} &= \mathrm{kron}(J_2\vec{n}_{\mathrm{t}}, J_2) \\ \partial_{\mathrm{t}} &= (\partial_x \;\; \partial_y)^{\mathrm{T}}, \quad n_{\mathrm{t}} = (n_x \;\; n_y)^{\mathrm{T}}\end{aligned} \tag{7}$$

$$J_2 = \begin{pmatrix}0 & 1 \\ -1 & 0\end{pmatrix}, \quad J_4 = \mathrm{kron}(J_2, J_2)$$

$$= \begin{pmatrix}0 & 0 & 0 & 1 \\ 0 & 0 & -1 & 0 \\ 0 & -1 & 0 & 0 \\ 1 & 0 & 0 & 0\end{pmatrix} = J_4^{-1} = J_4^{\mathrm{T}}. \tag{8}$$

$\vec{n}_{\mathrm{r}} = \vec{k}_{\mathrm{r}}/k_0$, $k_0 = \omega/c$, the superscript † indicates the hermitian conjugation, the elements γ_{ij} $(i, j = x, y, z)$ of γ_{tt}, γ_{zt}, γ_{tz} are the following 2×2 matrices

$$\gamma_{ij} = \begin{pmatrix}\varepsilon_{ij} & \chi_{ij} \\ \eta_{ij} & \mu_{ij}\end{pmatrix} \tag{9}$$

and $\mathrm{kron}(A, B)$ is the matrix having elements $a_{ij}B$ (Kronecker or tensor product).

Lossless and Lorentz-reciprocal media satisfy the Onsager–Casimir relations $\gamma_{ij} = \gamma_{ij}^{\dagger}$. This implies:

$$L = L^{\dagger} \tag{10}$$

which in turn implies the conservation of the energy flux through the planes $z = const.$ In fact that the z-component of the Poynting vector is proportional to $\psi^{\dagger}J_4\psi$, and the z-derivative of this quantity is equal to zero, is easily shown by expressing the derivative $\partial_z\psi^{\dagger}$ and $\partial_z\psi$ through equation (4) and considering equation (10).

The simple form of equation (4) and the symmetry of the quantities appearing in the propagation matrix L have been of great help in approaching the problem of its integration, i.e. to develop the algorithm and to write the codes.

3. The Standard Grating Method

The field generated by a plane wave incident on the LC sample is expressed as

$$\psi(\vec{r}_{\mathrm{t}}, z) = \int \vec{\psi}(\vec{k}_{\mathrm{t}}, z)\exp(\mathrm{i}\vec{k}_{\mathrm{t}}\vec{r}_{\mathrm{t}})\,\mathrm{d}\vec{k}_{\mathrm{r}}. \tag{11}$$

The starting point of our numerical analysis is to substitute the double integral over $\vec{k}_{\mathrm{t}}$ with the double summation

$$\psi(\vec{r}_{\mathrm{t}}, z) = \sum_{\vec{q}} \psi_{\vec{q}}(z)\exp[\mathrm{i}k_0(\vec{n}_{\mathrm{t,inc}} + \vec{q})\vec{r}_{\mathrm{t}}] \tag{12}$$

where $k_0\vec{n}_{\mathrm{t}}$ is the transverse component of the incident wave vector and the vector $k_0\vec{q}$ is regularly discretized as follows:

$$k_0\vec{q}_{m_x,m_y} = m_x\frac{2\pi}{p_x}\hat{x} + m_y\frac{2\pi}{p_y}\hat{y} \tag{13}$$

where m_x and m_y are integer numbers. The discretization means that we multiply $\vec{\psi}(\vec{k}_t, z)$ by a double Dirac's comb, and therefore convolute $\psi(\vec{r}_t, z)$ by the inverse Fourier Transform of this Dirac's comb, which is again a Dirac's comb defined on the points $m_x p_x \hat{x} + m_y p_y \hat{y}$. This operation generates a function periodic with respect to x and y, i.e. a 2D grating with periods p_x and p_y. For a laterally rectangular sample with periodic boundary conditions, p_x and p_y are identified with the lateral dimensions of the sample, as is evident. In the absence of periodic boundary conditions the function defining the grating becomes discontinuous, a fact that could give difficulties for the integration of the Maxwell equations. Inserting equation (12) into (4), one straightforwardly obtains

$$\partial_z \psi_{\vec{q}} = \mathrm{i} k_0 J_4 L_{\vec{q}\vec{q}'} \psi_{\vec{q}'} \tag{14}$$

where the summation over a repeated index is implicit,

$$L_{\vec{q}\vec{q}'} = \tilde{g}_{\mathrm{tt},\vec{q}-\vec{q}'} - N_{\vec{q}} \tilde{g}_{\mathrm{zt},\vec{q}-\vec{q}'} - \tilde{g}_{\mathrm{tz},\vec{q}-\vec{q}'} N^{\mathrm{T}}_{\vec{q}'} - N_{\vec{q}} \tilde{g}_{zz,\vec{q}-\vec{q}'} N^{\mathrm{T}}_{\vec{q}'} \tag{15}$$

and $\tilde{g}_{\mathrm{tt},\vec{q}}$, $\tilde{g}_{\mathrm{tz},\vec{q}}$, $\tilde{g}_{\mathrm{zt},\vec{q}}$ and $\tilde{g}_{zz,\vec{q}}$ are the matrices whose elements are the Fourier transforms of the 2×2 matrices $\gamma_{ij} - \gamma_{iz}\gamma_{zz}^{-1}\gamma_{zj}$, $\gamma_{iz}\gamma_{zz}^{-1}$, $\gamma_{zz}^{-1}\gamma_{zi}$, γ_{zz}^{-1}, respectively (with i and j running over x and y), and $N_{\vec{q}}$ is defined similarly to n_t, equation (7), with n_x and n_y substituted by $n_x + q_x$ and $n_y + q_y$. The equations (14), (15) are the extension to 2D bianisotropic gratings of the well known equations valid for 1D dielectric gratings [5].

Outside the grating each $\vec{q}$-value corresponds to a diffracted beam containing 4 independent plane waves, two transmitted and two reflected. Only a limited number M of beams is considered in the computations. Inside the grating it is convenient to make use of a staircase approximation along z, i.e. to treat the sample as a cascade grating made of z-independent layers. Within each layer the equation system (14) will be written in the compact form

$$\partial_z \Psi(z) = \mathrm{i} k_0 B \Psi(z) \tag{16}$$

where $\Psi(z)$ is the 4M-vector containing the 4-vectors $\psi_{\vec{q}}(z)$, corresponding to the diffraction orders, $B = J L_{\vec{q}}$, where J is the Kronecker product of the $M \times M$ identity matrix and J_4, $L_{\vec{q}}$ is a $4M \times 4M$ matrix containing the matrices $L_{\vec{q}\vec{q}'}$, with $L_{\vec{q}\vec{q}}$ along the main diagonal. The number M of diffraction orders must be at least equal to the number Q of non-negligible matrices $L_{\vec{q}\vec{q}'}$, but it could be much greater. In this last case the matrix $L_{\vec{q}}$ is sparse. The matrices $L_{\vec{q}\vec{q}'}$ with $\vec{q} \neq \vec{q}'$ play the role of coupling terms (coupled-wave approach).

Within each layer the system matrix B does not depend on z, and equation (16) can be easily integrated, giving

$$\psi(z + \Delta z) = U \psi(z), \tag{17}$$

where

$$U = \exp[\mathrm{i} k_0 B \Delta z] \tag{18}$$

is the transfer matrix of the layer and Δz its thickness. The transfer matrix of the cascade grating is the product of the transfer matrices associated with its layers.

4. Grating Method: perturbative approach

The CPU time required to compute the exponential function U appearing in equation (17) becomes prohibitive if the dimension $4M$ of the matrices is of the order of a thousand or greater. We develop here a method that can decrease the time by one order of magnitude or more, requiring the following operations:

(1) a transformation in the Hilbert space of the state vectors ψ, such as to give to the system matrix the structure of a quasi-diagonal matrix;
(2) a perturbation expansion with respect to the matrix containing the off-diagonal elements.

For the first operation it is enough to define a new state vector α whose elements are the amplitudes of the $4M$ plane waves with $\vec{k}_t = k_0(\vec{n}_{t,\mathrm{inc}} + \vec{q}_{m_x,m_y})$, propagating in a suitably chosen homogeneous medium. In our analysis we have chosen as the homogeneous medium the one defined by the zero order Fourier component of the tensor $\gamma(\vec{r})$.

After this transformation the system matrix is written as $A + a$, where A is diagonal and a contains its off-diagonal elements. The elements of A have the meaning of z-components of the normalized wave vectors associated with the plane waves propagating in the average medium. For usual LC pixels, their order of magnitude is 1, whereas the elements of the matrix a are at least one order of magnitude smaller.

The transfer matrix

$$U_\alpha = \exp[\mathrm{i} k_0 (A + a) \Delta z] \tag{19}$$

is now expanded in a power series of the elements of a, making use of equations similar to those appearing in the Baker–Campbell–Hausdorff formula [12]. More precisely we make use of the following expansion:

$$\exp[X + x] = \sum_{n=0}^{\infty} \sum_{m=n}^{\infty} \frac{1}{m!} \xi_{mn} \tag{20}$$

where

$$\xi_{m0} = X^m; \quad \xi_{m,m} = x^m \tag{21}$$

and the other elements $\xi_{m,n}$ are given by the recurrent relations

$$\xi_{m+1,n} = x \xi_{m,n-1} + X \xi_{m,n}. \tag{22}$$

The index n defines the multiplicity of the scattering events in the considered layer. The terms with $n = 0$ refer

to the average (homogeneous medium), and their sum is equal to $\exp[X]$, that is quickly computed because the matrix X is diagonal. The terms with $n=1$ depend linearly on the perturbative matrix x. By increasing n, an increasing number of products of square matrices is required. It is therefore convenient to stop the expansion at the orders one or two. These approximations generally require a further division of each layer into sub-layers. Typically, Δz is of the order of one wavelength and about 30 terms must be retained to compute the matrix U by a truncated Taylor series, each one requiring a matrix product. A better accuracy can be obtained by a first order perturbative expansion if we divide the layer into $2^3=8$ identical sub-layers. Their transfer matrix U_1 is very quickly computed, and the computation of U requires only three matrix products.

The scattering matrix of the whole sample, between the planes $z=0$ and $z=d$, can be computed by dividing its transfer matrix into four $2M\times 2M$ sub-matrices as follows:

$$U_g(d^+,0^-)=\begin{pmatrix} U_{11} & U_{12} \\ U_{21} & U_{22} \end{pmatrix} \tag{23}$$

where U_g is the transfer matrix obtained by choosing as independent variables the amplitudes of the plane waves propagating in the external media (the glasses) and the indices 1 and 2 refer to the progressive and regressive waves, respectively. The vectors $\alpha_t\equiv\alpha_1(d^+)$ and $\alpha_r\equiv\alpha_2(0^-)$ defining the transmitted and reflected fields are given by [5]:

$$\begin{pmatrix}\alpha_t\\ \alpha_r\end{pmatrix}=\begin{pmatrix} U_{11}-U_{12}U_{22}^{-1}U_{21} & U_{12}U_{22}^{-1} \\ -U_{22}^{-1}U_{21} & U_{22}^{-1}\end{pmatrix}\begin{pmatrix}\alpha_i\\ 0\end{pmatrix} \tag{24}$$

where $\alpha_i\equiv\alpha_1(0^-)$ defines the incident field at $z=0^-$. The zero at the left side of this equation corresponds to waves incident on the surface $z=d$, not considered here. However they could be present if the cell is a part of a more complex structure.

The use of equation (24) requires the inversion of the $2M\times 2M$ matrix U_{22}, that can be avoided by the following iteration procedure:

$$\begin{aligned} &\alpha_t^{(1)}=U_{11}\alpha_i; && \alpha_r^{(1)}=\bar{U}_{21}\alpha_t^{(1)};\\ &\alpha_t^{(2)}=\ldots\alpha_t^{(1)}+U_{12}\alpha_r^{(1)}; && \alpha_r^{(2)}=\ldots\bar{U}_{21}\alpha_t^{(2)};\end{aligned} \tag{25}$$

where $\bar{U}_{ij}$ $(i,j=1,2)$ are the four block elements of the inverse transfer matrix $U_g(0^-,d^+)=U_g^{-1}(d^+,0^{-1})$, that can be computed by the same method used to compute $U_g(d^+,0^-)$; $\alpha_t^{(1)}$ is the forward part of field $\alpha(d^+)$ computed by setting $\alpha(0^-)=\alpha_i$ (i.e. by neglecting the reflected field); $\alpha_r^{(1)}$ is the backward part of the field obtained by propagating back the vector $\alpha_t^{(1)}$ to the input interface, and so on. For all the samples considered here convergence is already reached at the step $\alpha^{(3)}$.

5. Grating Method: Reduced Order Algorithm

For the computation of the scattering matrix most of the computer time is spent in the products of square matrices. Such products can be completely avoided if we only look for the output field generated by a single incident field, ψ_i, that can be a plane wave or a superposition of plane waves. In fact for each one of the layers defined in § 3, the propagation equation (16) is immediately integrated, giving

$$\psi(z+\Delta z)=\exp[ik_0B\Delta z]\psi(z)=\sum_{n=0}^{\infty}\frac{1}{n!}(ik_0B\Delta z)^n\psi(z), \tag{26}$$

whose computation only requires the product of matrices by vectors.

The continuity of the vector ψ through the boundary planes allows us to find $\psi(d^+)$ if $\psi(0^-)$ is known. The difficulty arising from the fact that this last quantity is not known, owing to the presence of the reflected field, can be solved by the same iteration algorithm defined at the end of the preceding section.

For the computation of the summation appearing in equation (26), truncated at any given order, a reduced order method has been recently developed [6] that will be briefly summarized here. It proceeds through the following two steps.

The vectors ψ_n associated with the terms of a truncated series expansion (Krylov vectors) are strongly linear dependent. This means that all these vectors are practically contained in vector space (Krylov space) whose dimensionality K is very small ($\leqslant 10$). A standard algorithm, referred to as Singular Value Decomposition (SVD) [13], allows K to be found and to generate an orthonormal basis $\psi_1,\ldots,\psi_K$ in the Krylov space. The propagation equation can therefore be written as

$$\partial_z\psi^{(K)}=ik_0B_K\psi^{(K)} \tag{27}$$

where

$$\psi^{(K)}=U_K^{\dagger}\psi,\quad B_K=U_K^{\dagger}BU_K. \tag{28}$$

The columns of the transformation matrix U_K, that project the vectors and the matrices from the Hilbert to the Krylov space, are the vectors $\psi_1,\ldots,\psi_K$. Equation (27) is very quickly integrated, so that most of the CPU time is spent on the products required to generate the Krylov vectors.

The second step is by far the more important one, because it allows us to avoid the use of the big system matrix B. This fact is related to the very structure of the

matrices $L_{\vec{q}\vec{q}'}$. It is such that the product of the system matrix $B \equiv JL$ by a vector ψ is fully equivalent to the convolution of suitably defined vectors v_i ($i = 1, 6$) by ψ. To this purpose we recall that for full 3D samples the dimension of the Hilbert space could be of the order of 10^6. In such space it becomes impossible not only to manage square matrices, but even to store their elements in the RAM memory. However all the elements of the matrix L are defined by the $4Q$-dimensional vectors $N_{\vec{q}}$ and $\gamma_{ij,\vec{q}}$, as shown in equation (15). To realize the fact that the matrix product $B\psi$ is equivalent to the convolution of two vectors, it is enough to insert equation (15) into (14). One obtains an expression containing summations over $\vec{q}'$ of terms of the type $v_{\vec{q}-\vec{q}'}\psi_{\vec{q}'}$, i.e. convolution products.

The definition of the vectors v_i is given in [6]. We only stress here the following point: the direct convolution of two vectors requires the same number of multiplications as the product of a square matrix by a vector, but in the Fourier-transformed space the convolution becomes the usual element-by-element product of two vectors, a fact that allows the CPU time to be greatly reduced.

6. Finite Difference in Frequency Domain Method

The direct integration of the Markuvitz–Schwinger equation in real space has been performed by writing the following set of equations for the vectors $\psi_{ij}(z)$ which define the electromagnetic field at the points x_i, y_j of the discretized specimen:

$$\partial_z \psi_{ij} = \mathrm{i}k_0 J_4 L_{ij,i'j'} \psi_{i'j'} \tag{29}$$

where the matrices $L_{ij,i'j'}$ with $i = i'$ and $j = j'$ contain the values for the material parameters in points (x_i, y_j) and the others, acting as coupling matrices, are defined by the well known finite difference matrix operators [14], which for periodic boundary conditions have a very simple structure.

The equation set (29) can be written in the compact form of equation (16). The system matrix B is here very sparse and therefore easily stored and treated.

The same perturbation method defined in § 4 can be applied here, but it is generally less convenient. In fact the elements of the derivative matrices are small with respect to 1 only if the space discretization step is very large, of the order of one wavelength.

For the Reduced Order Method the product of $B\psi$ can no longer be substituted by a convolution product; nevertheless it is quickly computed because the matrix B is very sparse.

7. Applications: in-plane switching (IPS) LC cells

The methods developed in the preceding sections have been applied to IPS cells which are of strong interest for the realization of wide viewing angle displays [15–17]. We consider cells whose electrodes are transparent strips parallel to a given direction, say y, coated on one of the boundary planes. In the distorted (ON) state the strips are alternatively positive and negative. If they are equispaced, the cell behaves as a 1D grating with the grating wave vector along x.

The cell is illuminated by a large and incoherent source. In a plane-wave expansion of the incident field, the phases are therefore stochastic variables. We assume that the intensities $I_{\mathrm{inc},j}$ of these plane waves are well defined functions of their direction and that the phases are randomly and uniformly distributed over the entire angle 2π. With such an assumption, the average output intensity $\langle I_i \rangle$ of the i-wave is given by

$$\langle I_i \rangle = |S_{ij}|^2 I_{\mathrm{inc},j} \tag{30}$$

where S is the scattering matrix of the cell. We have computed the total output intensity I_{tot} and its angular distribution $I(\theta)$ for a cell between crossed polarizers, under the simplifying assumption that all the wave vectors are parallel to a given plane, so that a single angle θ is enough to define their directions. For comparison of the numerical methods being considered such an assumption is not strongly restrictive. A more complete analysis of the performances of large LC cells is in progress and will be published in a future paper.

Instead of considering a particular cell, we tested the methods with a director distribution which is characterized as follows. The average director orientation is defined by the polar coordinates Θ and Φ with respect to a cartesian frame having the z-axis normal to the sample and the other axes in the directions of the crossed polarizers. To define the Fourier composition of $\epsilon(\vec{r})$ we have assumed that $\hat{n}$ is non-uniformly rotating or oscillating around its average direction in such a way as to generate any chosen number Q of Fourier components. If the number M of incident plane waves is very large, the total transmitted intensity I_{tot} is practically independent of their phases and coincides therefore with its average value $\langle I_{\mathrm{tot}} \rangle$. The dependence of this quantity on the cell thickness d is plotted in figure 1 for $Q = 40$, $\Theta = 90^\circ$ and for two different values of Φ. The amplitudes of the Fourier components have been computed by assuming that $\hat{n}$ depends only on x and that it is non-uniformly rotating around its average direction on a cone with 18° of semi-aperture. The intensity I_{tot} has been normalized with respect to the total intensity incident on the cell, after the polarizer. The function $I(\theta)$ and its average value $\langle I(\theta) \rangle$ are shown in figure 2 (dots and solid line, respectively) for four values of the normalized thickness d/λ. The intensity of the incident plane waves has been assumed to be uniform in the

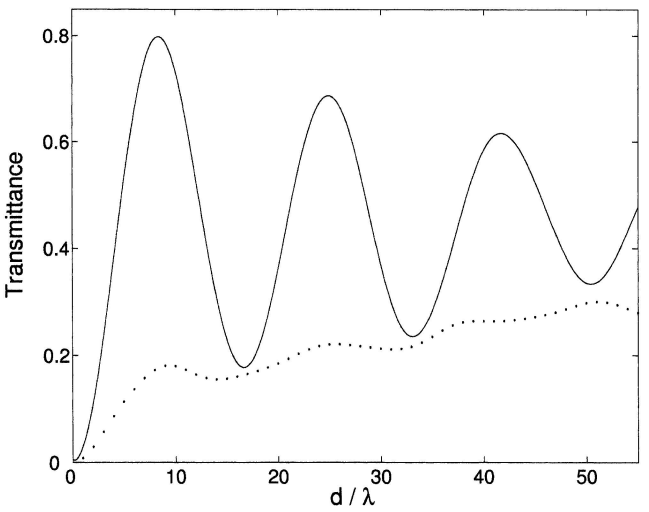

Figure 1. Transmittance vs. normalized thickness of a cell with refractive indices $n_e = 1.66$, $n_o = 1.54$ between crossed polarizers. Dotted line: $\Theta = 0$ and $\Phi = 0$, solid line: $\Theta = 0$ and $\Phi = 18^\circ$ where Φ is the azimuthal angle between the polarizer and the average director orientation.

interval $-62^\circ < \theta < 62^\circ$ and zero outside, to make more evident the effect of the cell on the angular distribution of the transmitted light.

The computations can be done by any one of the previously defined methods, which are numerically exact. The different methods are discussed in the next section. Here we only observe that our analysis confirms that the IPS cells can be efficient; shows that the diffraction, which has been neglected in [16, 17], could play a non negligible role; and suggests that it could be possible to obtain wide viewing angles without the use of a compensator.

8. Comparison of different methods and concluding remarks

With reference to the plots of figures 1 and 2, the perturbative approach to the GM is the most convenient because it allows us to compute the entire scattering matrix. It requires four minutes to compute all the plots of figure 2, where the number M of beams is equal to 241. The CPU times for the different versions of the GM are shown in figure 3, for different values of M and for $Q = 45$, where Q is the number of Fourier components. For $Q/M \ll 1$ the perturbative approach requires times increasing nearly linearly with M and Q. For higher Q-values their dependence on M and Q becomes more complex and more drastic. It is worthwhile observing that it has never been necessary to consider evanescent waves because an incidence angle of 90° in air corresponds to angles smaller than 45° in the LC cell.

The times required by the FDFD methods depend essentially on the number of the grid points (x_i, y_i) and on the sample thickness. However the spacing of the grid points strongly depends on the thickness d, on the smoothness of the director profile and on the input field, that can be a single plane wave or a superposition of plane waves. The distance between the grid points can range from $\lambda/20$ to λ or more. The dependence of the CPU time on this last parameter (for fixed cell dimensions) is so strong that a plot similar to that of figure 3 is of small interest. In general, the times required by this method are larger than those required by the GM. We only observe that the number of non-zero elements of the system matrix B, that is quasi-diagonal, increase linearly with N, which in turn increases linearly with the lateral dimensions of the cell. On the contrary, the number of non-zero elements of the system matrix for the GM increases linearly with both M and Q, and therefore quadratically with the lateral dimensions of the cell. The increase becomes linear only by using the reduced order GM defined in 5.

Let us conclude with the following observations. The main motivation of this research is the study of LC cells with strong lateral variation of the director field, devices of increasing interest for the realization of wide viewing angle displays. In the LC literature the transmittance of large cells is usually computed using approximate methods which neglect diffraction, and the optimization of the cells is generally obtained by performing experiments. The methods defined here allow us to approach this problem of optimization using numerical simulations, assuming that we know the director field $\hat{n}(\vec{r})$ (the function $\hat{n}(\vec{r})$ can be computed making use of commercial software or the methods recently developed by Fernandez and co-workers [18]). The GM method is generally the most suitable. Using the perturbative method it is possible to compute in a reasonable time the scattering matrix of the 2D pixels (having dimensions of a few hundred micrometers) actually used in LC displays. Full 3D cells require instead the use of the reduced order method, that has been usefully applied to $80 \times 80 \times 5\,\mu m^3$ or smaller cells for a given input. Further improvements of the GM, which are under study, are required to treat larger cells. However it must be observed that the problem of cell optimization could be solved using smaller cells and correctly taking into account the diffraction effects, which depend on the sample size.

As is evident, interest in the numerical methods developed here goes well beyond the optics of liquid crystals. According to our analysis, the GM is generally preferable for samples between parallel planes and with laterally periodic boundary conditions. For non-periodic boundary conditions the functions defining the material parameters become discontinuous. For the GM a large number of Fourier components is then required, a fact

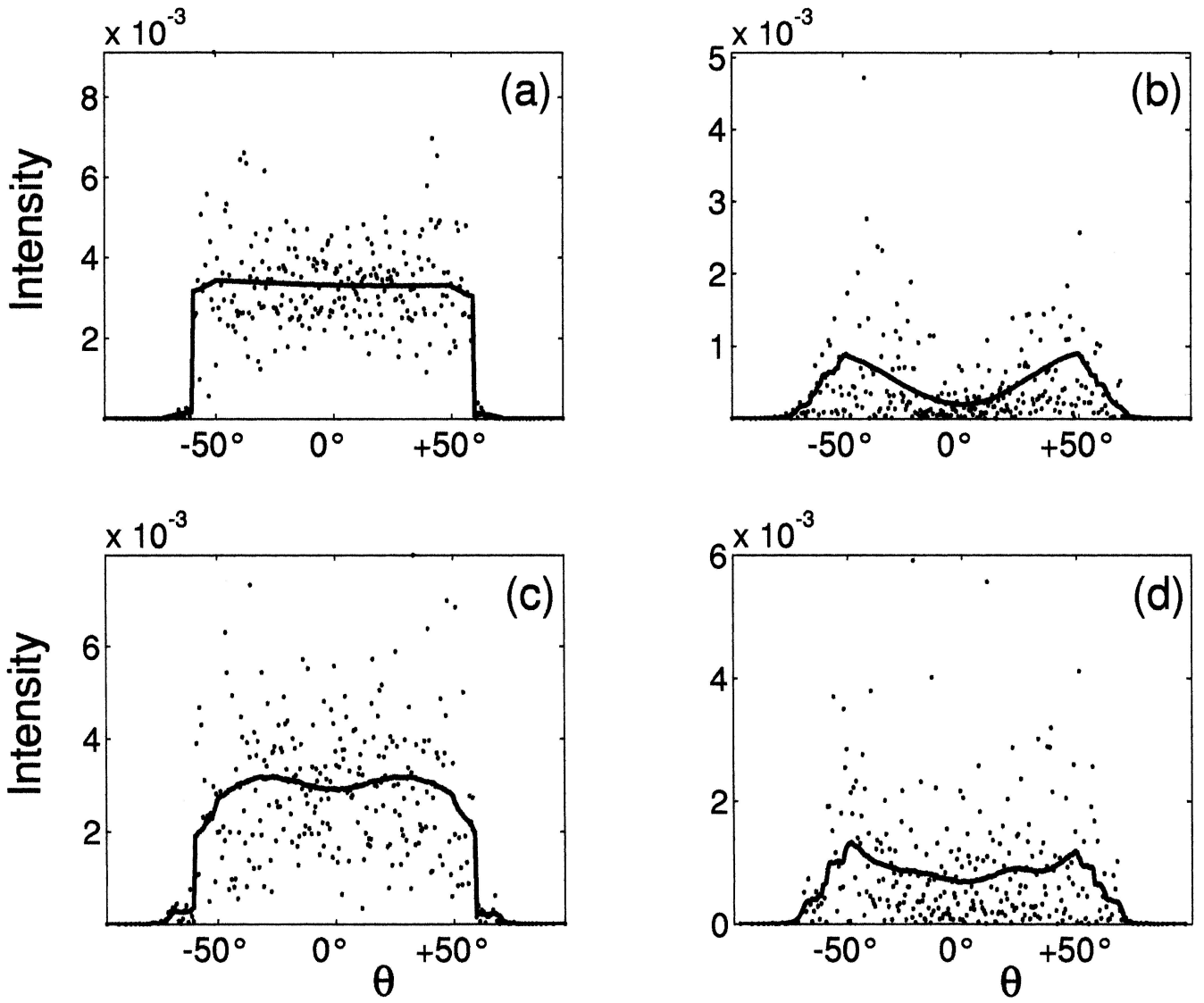

Figure 2. Angular distribution of the transmitted intensity, for incident light with intensity uniformly distributed in the θ-interval $(-62^\circ, 62^\circ)$ and random phases. Sub-plots (*a*), (*b*), (*c*), (*d*) correspond to $d/\lambda = 8$, 16, 24 and 32, respectively (the maxima and minima of the solid line in figure 1). The dots refer to an incident field with random phases, and the solid line to their average over all the possible phases.

that increases the dimension of the Hilbert space. The discontinuities could be more easily and quickly managed with the FDFD method.

Moreover, the formulation of the FDFD method given in § 6 is particularly suitable for generating several, very important approximations, of which the following are recalled.

(i) By dropping the matrices associated with the transverse derivatives, all the coupling matrices $L_{ij,i'j'}$ with $i \neq i'$ and $j \neq j'$ appearing in equation (29) go to zero and the decoupled equations are those used by the standard Berreman method. An improved version of this last method can be obtained by retaining the transverse derivatives of $\gamma(\vec{r})$ and neglecting those of the state vector $\psi(\vec{r}_t, z)$. Since only these last derivatives couple the 4×4 matrices associated with the grid points, the integration of the improved Berreman matrices, which take into account the transverse variation of the material parameter, is as simple as for the standard method.

(ii) By further dropping the coupling between progressive and regressive waves one obtains the standard Jones matrix method, or its improved version that takes into account the transverse derivative of $\gamma(\vec{r})$.

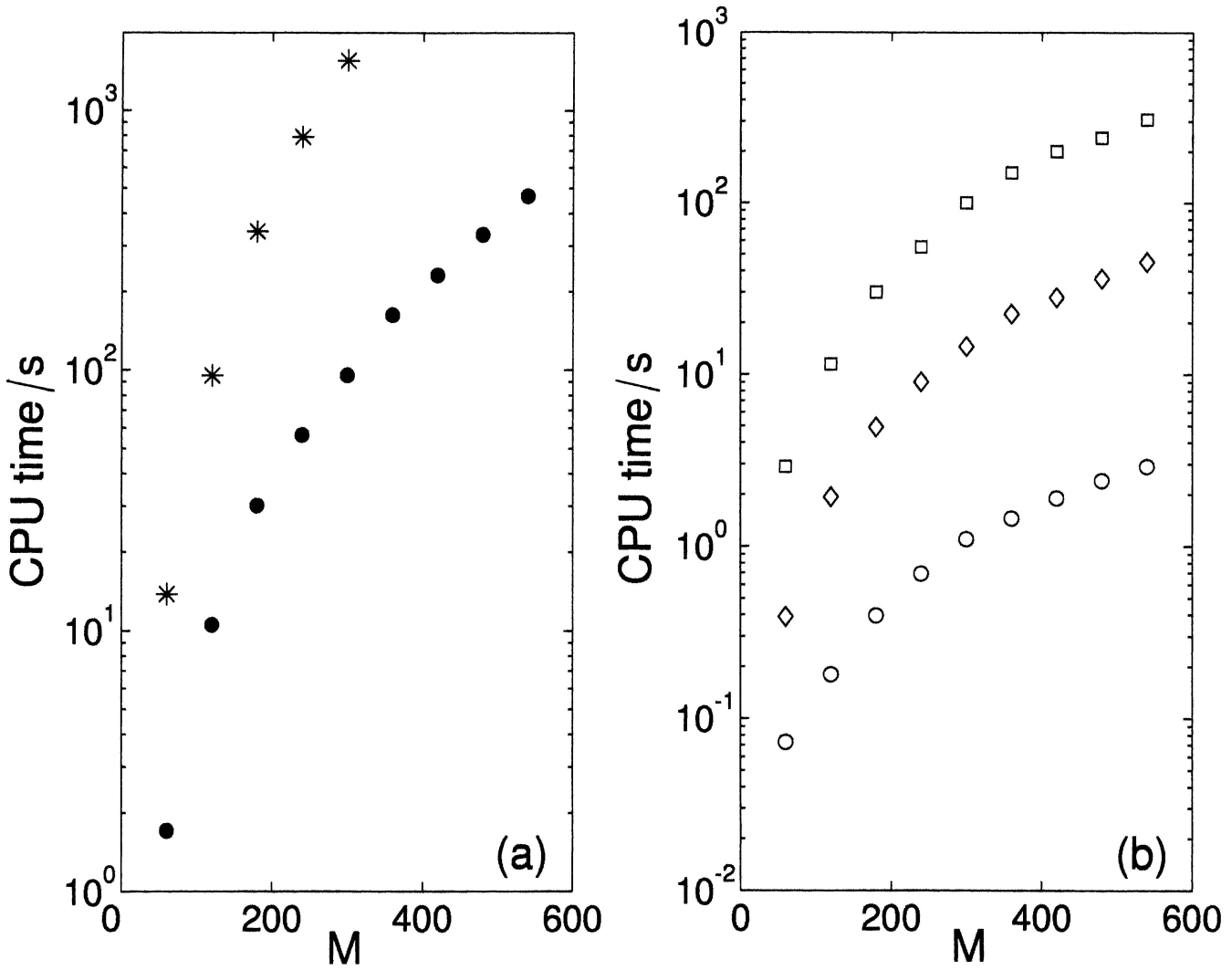

Figure 3. (*a*) CPU time for the computation of the transfer matrix U vs. the number M of diffracted beams: the asterisks refer to the standard GM, the dots to the GM with the perturbation algorithm. (*b*) CPU time for the computation of the output field for a given input vs. M, using standard (squares), perturbative (diamonds) and reduced order (circles) methods.

The improved methods always give better results than the standard methods, in particular for very thin samples ($d \approx \lambda$). They can be used to obtain an improved Beam Propagation Method (BPM) based on the division of the sample into thin layers.

We finally recall that all the equations given here can be applied to magnetic, chiral and bianisotropic media, thus allowing extension to more complex media of the exact as well as the approximate methods already developed for dielectrics.

We thank Dr D. de Boer, Dr H. Woehler and Prof. D. Iordache for useful suggestions. Part of this work has been supported by European Commission, project G5RD-CT 1999-00115.

Appendix: list of symbols

A^{T} transpose of A.
$A^{\dagger}$ transpose hermitian of A.
$\hat{n}(\vec{r})$ director field.
$\vec{r}_{\mathrm{t}}$ transverse part of $\vec{r}$, ($\vec{r} = \vec{r}_{\mathrm{t}} + \hat{z}$).
J_4 exchange matrix.
$J_4 L$, 4×4 Marcuvitz–Schwinger matrix.
$J_4 L_{\vec{q}\vec{q}'}$, 4×4 system matrix in the spectral domain.
$J_4 L_{ij,i'j'}$, 4×4 system matrix in the FDFD formalism.
M number of diffracted beams.
$B = JL$, $4M \times 4M$ system matrix.
S scattering matrix.
U, U_{g}, U_{α} transfer matrices.
Z_0 vacuum characteristic impedance.
$\gamma, \gamma_{ij}, \ldots$ matrices defining the material parameters.

$\tilde{g}, \tilde{g}_{ij}, \ldots$ Fourier transforms of $\gamma, \gamma_{ij}, \ldots$.
$\psi(\vec{r})$ state 4-vector.
$\psi_{\vec{q}}(z)$ state 4-vector for the $\vec{q}$ spectral component.
$\Psi(z)$ state $4M$-vector in the spectral domain.
$\psi^{(K)}$ state vector in the Krylov space.
$\psi_{ij} = \psi(x_i, y_j)$ state vectors for the FDFD method.

References

[1] Budden, K. G., 1966, *Radio Waves in the Ionosphere* (Cambridge: Cambridge University Press).
[2] Berreman, D. W., 1972, *J. opt. Soc. Am. A*, **62,** 502.
[3] Yeh, P., and Gu, C., 1999, *Optics of Liquid Crystal Displays* (New York: Wiley).
[4] Mueller, H., 1948, *J. opt. Soc. Am. A*, **38,** 661.
[5] Rokushima, K., and Yamakita, J., 1983, *J. opt. Soc. Am. A*, **73,** 901.
[6] Peverini, O. A., Olivero, D., Oldano, C., de Boer, D. K. G., Cortie, R., Orta, R., and Tascone, R., 2002, *J. opt. Soc. Am. A*, **19,** 1901.
[7] Taflove, A., 1995, *Computational Electrodynamics: The Finite-Difference Time-Domain Method* (Norwood: Artech House).
[8] Kriezis, E. E., and Elston, S. J., 2000, *Appl. Opt.*, **39,** 5707.
[9] Lindell, J. V., Sihvola, A. H., and Suchy, K., 1995, *J. Electromagn. Waves Appl.*, **9,** 887.
[10] Sjberg, D., 2000, *Wave Motion*, **32,** 217.
[11] Marcuvitz, N., and Schwinger, J., 1951, *J. appl. Phys.*, **22,** 806.
[12] Gilmore, R., 1974, *Lie Groups, Lie Algebra, and Some of Their Applications* (New York: Wiley).
[13] Dammel, J., Ming, G., Eisenstat, S., Slapnicar, I., Veselic, K., and Drmac, Z., 1999, *Linear Algebra Appl.*, **299,** 21.
[14] Mitchell, A. R., and Griffiths, D. F., 1980, *The Finite Difference Method in Partial Differential Equations* (New York: Wiley).
[15] Aratani, S., Klausmann, H., Oh-e, M., Ohta, M., Ashizawa, K., Yanagawa, K., and Kondo, K., 1997, *Jpn. J. appl. Phys.*, **36,** 27.
[16] Anderson, J. E., and Bos, P. J., 2000, *Jpn. J. appl. Phys.*, **39,** 6388.
[17] Hong, S. H., Kim, H. Y., Lee, M. H., and Lee, S. H., 2002, *Liq. Cryst.*, **29,** 315.
[18] Fernandez, F. A., Day, S. E., Trwoga, P., Deng, H. F., and James, R., *Mol. Cryst. Liq. Cryst.* Proceedings of OLC2001, 9th Int. Topical Meeting on Optics of Liquid Crystals, Sorrento, Italy, 1–6 Oct. 2001, 77.